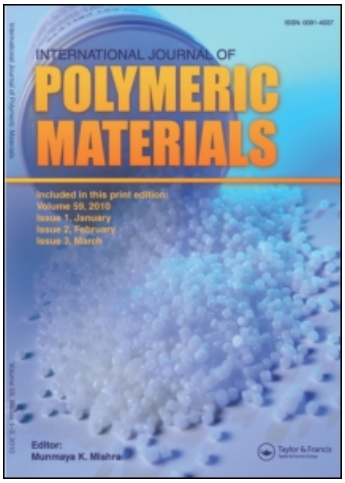

International Journal of Polymeric Materials
Publication details, including instructions for authors and subscription information:
http://www.informaworld.com/smpp/title~content=t713647664

Hydroxyapatite-Reinforced Polyamide 6,6 Nanocomposites through Melt Compounding

Deepthy Menon[a]; K. Anoop Anand[a]; V. C. Anitha[a]; Shantikumar Nair[a]
[a] Amrita Centre for Nanosciences and Molecular Medicine, Amrita Vishwa Vidyapeetham, Amrita Institute of Medical Sciences and Research Centre, Cochin, Kerala, India

Online publication date: 13 May 2010

To cite this Article Menon, Deepthy , Anoop Anand, K. , Anitha, V. C. and Nair, Shantikumar(2010) 'Hydroxyapatite-Reinforced Polyamide 6,6 Nanocomposites through Melt Compounding', International Journal of Polymeric Materials, 59: 7, 498 — 509
To link to this Article: DOI: 10.1080/00914031003627262
URL: http://dx.doi.org/10.1080/00914031003627262

International Journal of Polymeric Materials, 59:498–509, 2010

ISSN: 0091-4037 print/1563-535X online
DOI: 10.1080/00914031003627262

Taylor & Francis
Taylor & Francis Group

Hydroxyapatite-Reinforced Polyamide 6,6 Nanocomposites through Melt Compounding

Deepthy Menon, K. Anoop Anand, V. C. Anitha, and Shantikumar Nair

Amrita Centre for Nanosciences and Molecular Medicine, Amrita Vishwa Vidyapeetham, Amrita Institute of Medical Sciences and Research Centre, Cochin, Kerala, India

Hydroxyapatite-reinforced polyamide 6,6 nanocomposites were prepared for load-bearing bone implant applications. Nanoparticles of hydroxyapatite (nHAp) were synthesized through a wet chemical reaction and were incorporated into the polymer melt at different loading fractions by melt compounding so as to sensitively modulate the mechanical properties of the latter. Tensile properties of the nanocomposites were found to be substantially improved at filler loading fractions as low as 3 wt%. Theoretical calculations also confirm the improved extent of reinforcement for nanocomposites over the predicted data for conventional micro counterparts. Differential scanning calorimetry studies revealed that the melting and crystallization characteristics of the polyamide matrix were unaltered with the incorporation of nHAp. However, the addition of nanohydroxyapatite considerably influenced the thermal stability of the nanocomposites.

Keywords hydroxyapatite, implant, nanocomposites, polyamide

Received 28 December 2009; in final form 31 December 2009.
The authors are thankful to the Department of Science and Technology, Government of India, for financial support under the Nanoscience and Nanotechnology (NS & NT) initiative of the Government of India monitored by Prof. C. N. R. Rao.
Address correspondence to Shantikumar Nair, Amrita Centre for Nanosciences and Molecular Medicine, Amrita Vishwa Vidyapeetham, Amrita Institute of Medical Sciences and Research Centre, Cochin 682 041, Kerala, India. E-mail: shantinair@aims.amita.edu

INTRODUCTION

Calcium phosphate ceramic materials have been used for skeletal tissue engineering applications because of their excellent biocompatibility and osteoconductive properties [1,2]. Among these materials, hydroxyapatite [HAp, $Ca_{10}(PO_4)_6(OH)_2$] is the major inorganic compound possessing similar chemical and crystal structure to that of bone mineral. Hydroxyapatite has been used for biomedical implant applications for the past several decades. Despite their biocompatibility and osteoconductivity, Hap-based ceramics, however, have limited clinical applications because of their brittleness and fatigue failure. Moreover, their high Young's modulus values cause stress shielding after implantation, which often results in bone resorption and loosening of implants [3,4]. Hence, attempts have been made to develop polymer matrix composites containing a particulate, bioactive component, which could eliminate stress shielding and interfacial loosening to a considerable extent [5]. Since natural bone can be considered as a collagen-apatite composite, such a system appears to be the natural choice for bone implants. The bioactive component of the composite renders bioactivity, whereas the matrix polymer will provide ductility and other associated properties required for hard tissue replacement biomaterials [6].

Hydroxyapatite-reinforced high-density polyethylene composite was the first bioactive ceramic–polymer composite designed to mimic the structure and properties of bone, reported in 1981 [7]. Later, bioglass-reinforced polyethylene [8] and glass–ceramic reinforced high-density polyethylene [9] have been reported. Though such systems exhibited appropriate mechanical compatibility to bone, unlike metals and ceramics, there exists less coupling between the nonpolar polymer matrix and the filler particles. Later, hydroxyapatite-reinforced ultrahigh molecular weight polyethylene [10,11], polysulfone [12], polyetheretherketone [13], poly(L-lactide) [14,15], and polyamide 6 [16] have also been reported. Nanohydroxyapatite (nHAp)-reinforced polyamide 6,6 (PA 6,6) biocomposites for load-bearing bone repair have been developed [17–20]. In this composite, prepared through coprecipitation method, nHAp particles retained their nanoscale features and were dispersed uniformly in the matrix. The mechanical properties of the composites were similar to that of natural bone for nHAp concentration of >65%. However, the methodology adopted by the authors consumes a large excess of solvent, which is not feasible from a commercial point of view.

Polyamide (PA), the polymer selected for the present investigation, has a structure similar to bone collagen, while nanohydroxyapatite has high surface activity and size similar to the mineral found in human hard tissues [21]. Moreover, nHAp takes advantage of a homogeneous distribution and chemical bonding within the polar PA matrix. Although nHAp-reinforced PA composite has good mechanical and biological properties, for clinical applications,

manufacturing processes must also be improved. So far, there have been no reports in the literature that adopts melt compounding as a possible means to fabricate PA 6,6-nHAp biocomposite materials for implant applications. In the work reported here, nHAp is used as the nanofiller at concentrations ranging from 0 to 10 wt% in polyamide matrix. Preliminary investigations are carried out to examine the effect of nHAp on the mechanical and thermal properties of polyamide 6,6.

EXPERIMENTAL

Materials

Polyamide 6,6 was purchased from Polysciences Inc., USA. Calcium hydroxide, $Ca(OH)_2$ was supplied by Merck India Pvt. Ltd., and phosphoric acid, H_3PO_4 was supplied by Qualigens India Pvt. Ltd.

Synthesis and Characterization of Nanohydroxyapatite

Hydroxyapatite nanoparticles were prepared by the wet chemical method using calcium hydroxide and phosphoric acid as Ca and P precursors, respectively [22]. Typically, 9.26 g $Ca(OH)_2$ was added to 250 mL distilled water and stirred at 100°C for 2 h. 0.3 M H_3PO_4 solution was added dropwise to this solution at a rate of ~2 mL/min. Addition of this acidic solution continued until the pH of the mixture dropped to 7.4. The reaction was then allowed to proceed at 100°C for another 2 h and then kept overnight at ambient. The supernatant was discarded and the precipitate was washed four times with hot water with subsequent centrifugation. The precipitate was dried at 60°C overnight under vacuum and then characterized. The chemistry involved in the synthesis is represented as follows:

$$10Ca(OH)_2 + 6H_3PO_4 \rightarrow Ca_{10}(PO_4)_6(OH)_2 + 18H_2O$$

Crystallinity of the sample was studied using an X–ray diffractometer [Rigaku Dmax-C] fitted with Cu-Kα ($\lambda = 1.541$ Å) source. The spectrum was recorded in the range of 20 to 80° with a step size of 0.05° and phase identification was carried out with the help of standard JCPDS database. A Nicomp particle size analyzer (Nicomp 380, Particle Sizing Systems, USA) which utilizes the technique of dynamic light scattering (DLS), was used for particle size analysis. The average particle size as well as the size distribution could be noted from this measurement. Spectroscopic evaluation of the synthesized HAp was carried out using a Fourier transform infrared spectrometer (FTIR) (Perkin Elmer Spectrum RX1) in the spectral range between 4000 and 400 cm^{-1}, with a resolution of 2 cm^{-1}. SEM images were obtained using a JEOL analytical

scanning electron microscope (JSM-6490 LA). The composition of the synthesized HAp was determined by energy dispersive spectral analysis, which was recorded using the EDAX attachment of SEM.

Preparation of the Nanocomposites

A simple melt compounding route was adopted for the preparation of polyamide 6,6-nHAp nanocomposites. The polymer and the filler were vacuum dried at 100°C for 6 h to avoid moisture. Melt compounding was performed using a Thermo Haake Minilab operating at 80 rpm (counter-rotating screws) for 10 min at 280°C. Nanocomposites at different concentrations (0–10 wt%) of nHAp were prepared. A mixing time of 10 min was fixed since the torque stabilized to constant values during this time, which might be related to the attainment of a stable nanocomposite structure.

In order to study the mechanical properties, the extruded samples were chopped to pellets using a fiber chopping system, further dried at 100°C for 4 h and then injection-molded using a Thermo Haake Minijet. The cylinder temperature of Minijet was maintained at 285°C and the mold temperature was kept at 100°C. The injection pressure was 400 bar (4 sec) and post-injection pressure was maintained at 300 bar (10 sec). Dumbbell shaped specimens were prepared by injection-molding.

Mechanical Properties

Mechanical properties of the injection-molded nanocomposite specimens were studied using a servo hydraulic materials testing system (MTS) with a load cell of 10 kN capacity. The gauge length between the jaws at the start of each test was adjusted to 30 mm and the measurements were carried out as per the relevant ASTM standards at a crosshead speed of 50 mm/min. The average of at least six sample measurements was taken to represent each data point.

Thermal Characteristics

Crystallization characteristics of the melt-compounded nanocomposites were studied by employing differential scanning calorimetry (Diamond DSC, Perkin Elmer). Indium was used for temperature calibration ($T_m = 156.6°C$, $\Delta H_m = 28.4\,J/g$). All the samples were dried prior to the measurements and analyses were carried out in nitrogen atmosphere using standard aluminum pans. Calorimetric measurements were done while the samples (6–8 mg) were exposed to the following ramp and hold cycles: (i) heating at 20°C/min to 300°C, (ii) hold for 10 min (to erase thermal history effects) and (iii) cooling

to 50°C at 20°C/min. During the cooling step, the peak of crystallization exotherm was taken as the crystallization temperature, T_c. The heat of fusion (ΔH_m) and heat of crystallization (ΔH_c) were determined from the areas of the melting and crystallization peaks, respectively.

Thermogravimetric Analysis

The effect of nanohydroxyapatite on the thermal stability of polyamide 6,6 was tested using thermogravimetric analysis (TGA, Q-50, TA Instruments) by heating ~5 mg of the sample from ambient temperature to 800°C at the rate of 20°C/min in nitrogen ambience (swept at 60 mL/min).

RESULTS AND DISCUSSION

The crystalline structure, chemical composition and morphological characterization of the synthesized hydroxyapatite nanoparticles, which is the nanofiller used in the current study, are discussed below along with their effect on the mechanical and thermal properties of the matrix polymer. A comparison of the mechanical properties of the nanocomposites is also made with the predicted data calculated on the basis of theoretical assumptions for the micro counterparts.

Characterization of nHAp

The crystalline phase structure of hydroxyapatite is depicted in the XRD spectrum shown in Figure 1. Nanohydroxyapatitite synthesized for preparing the PA-HAp composite revealed good crystallinity as evident from the XRD spectrum, with the prominent XRD peaks matching with the reported data [JCPDS data file (No. 090432)].

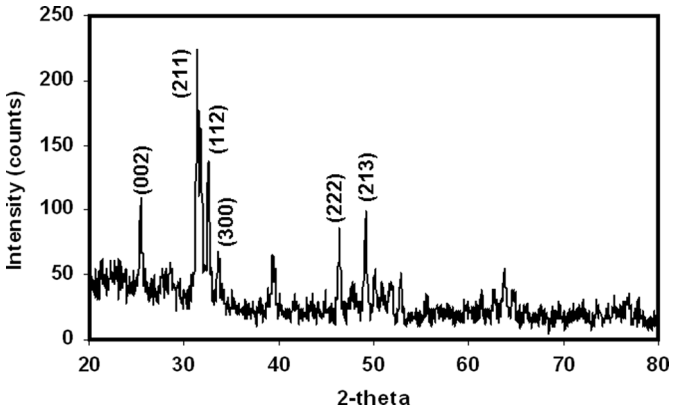

Figure 1: XRD spectrum of nanohydroxyapatite.

Figure 2 is the FTIR spectrum indicating the absorption peaks corresponding to the characteristic functional groups of HAp. As shown in the spectrum, the two bands at 3571 and 633 cm^{-1} represent the vibration of the hydroxyl group. The bands at 1031, 1094 and 963 cm^{-1} are the characteristic bands of phosphate stretching vibrations, whereas the bands at 603 and 565 cm^{-1} are due to the phosphate bending vibrations.

A typical scanning electron micrograph of the nanoparticles is given in Figure 3(a). A SEM image reveals that the nanoparticles are more or less monodispersed and are spherical with an approximate particle size of 80 nm. The energy-dispersive spectrum of the nanoHAp particles revealing the approximate ratio of Ca to P as 1.67 is represented in Figure 3(b).

Mechanical Properties of PA 6,6-nHAp Nanocomposites

The effect of nanohydroxyapatite on the mechanical properties of PA 6,6 is indicated in Table 1. From the results it is evident that the mechanical properties of the polymer matrix are substantially improved even at low concentrations of nHAp. For example, the tensile modulus of the nanocomposite sample containing nHAp at a concentration as low as 3.0 wt% is almost 50% higher than that of neat PA 6,6. Though the strength of the sample showed no considerable improvement at this loading fraction, elongation of the nanocomposite was reduced due to the embrittlement of the polyamide matrix.

The composite modulus of nanoparticle-reinforced matrices has been studied by using finite element analysis as well as other models such as the modified Cox [22] model and Halpin-Tsai equations [23,24]. The longitudinal modulus of aligned discontinuous fiber composites as a ratio with respect to the modulus of the matrix alone (E_c/E_m) proposed by Halpin is given by:

$$\frac{E_c}{E_m} = \frac{1 + \xi\eta v_f}{1 - \eta v_f} \tag{1}$$

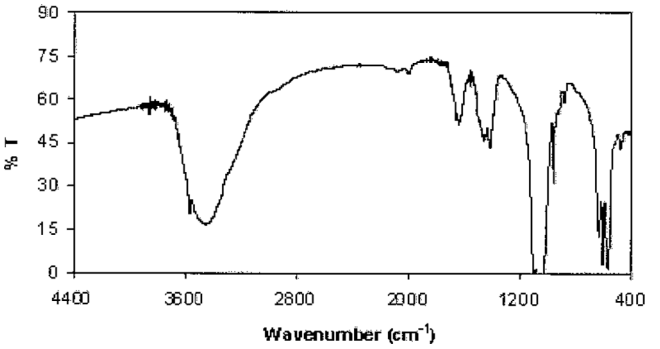

Figure 2: FTIR spectrum of nanohydroxyapatite.

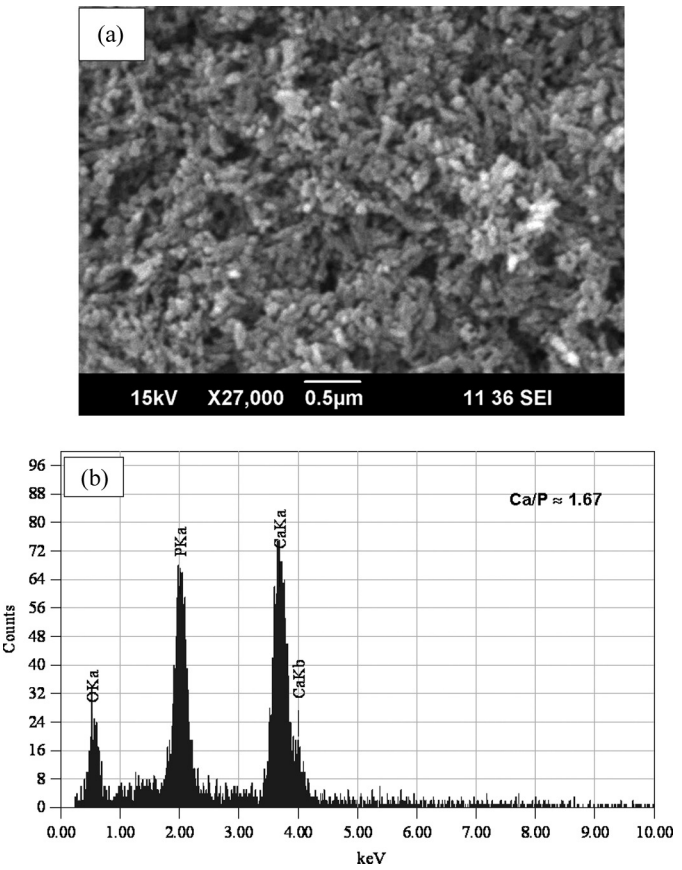

Figure 3: (a) SEM image and (b) EDAX of nanohydroxyapatite particles.

where,

$$\eta = \frac{(E_f/E_m) - 1}{(E_f/E_m) + \xi} \tag{2}$$

and E_c and E_m correspond to the modulus values of the composite and matrix, respectively. The value of $\xi = 2L/d$. For equiaxed particles, $L = d$ and hence the

Table 1: Mechanical properties of melt-compounded PA 6,6-nHAp nanocomposites.

Concn. of nHAp (wt%)	Concn. of nHAp (vol%)	Tensile strength ratio	Tensile modulus ratio (Experimental)	Tensile modulus ratio (Theoretical)	Elongation at break (%)
0	0	1	1	1	178.0
3	1.1	1.03	1.49	1.03	59.1
5	1.9	1.06	1.55	1.06	42.3
10	3.9	1.13	1.62	1.12	29.8

value of $\xi = 2$. In the above expressions, v_f represents the volume fraction of the filler and E_f the tensile modulus of the filler. In the present case, the filler is nanohydroxyapatite and matrix is polyamide. Considering $E_{HAp} = 114$ GPa and $E_{PA} = 0.69$ GPa [25] and for the experimental volume fractions used, the ratio of tensile modulus of the composite to that of the matrix polymer alone (E_c/E_m) was calculated theoretically for microparticles of hydroxyapatite using the above expressions and has been compared with the experimental tensile modulus ratio. A plot showing the variation of tensile modulus ratio with volume fraction for the nanoparticle-reinforced composite [PA 6,6-nHAp] and microHAp-reinforced polyamide matrix (theoretical) is given in Figure 4.

As is evident from the graph, the tensile modulus ratio increases considerably when a nanofiller is used for reinforcing the matrix as against that of microparticle-reinforced matrix. Typical stress-strain plots of neat PA 6,6 and PA 6,6-nHAp nanocomposites are also provided in Figure 5.

The improved mechanical properties of the nanocomposites as compared to neat polyamide are attributed to the efficient stress transfer from the matrix to the nHAp particles, which in turn might be correlated to the better dispersion of the nanoparticles in the polymer matrix. We assume that the high shear forces employed during the melt extrusion enabled better dispersion of nHAp in PA 6,6.

Thermal Characteristics

Differential scanning calorimetry has been extensively used to identify the effects of nanoparticles in the polymer matrix in changing the crystallization characteristics. In order to determine the effect of nanohydroxyapatite

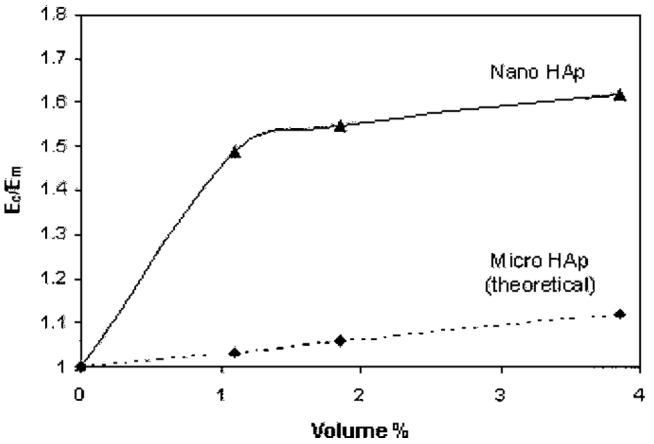

Figure 4: Comparison in variation of E_c/E_m with vol% for HAp particles (nano HAp – experiment and micro HAp – theory based on continuum model for microparticles).

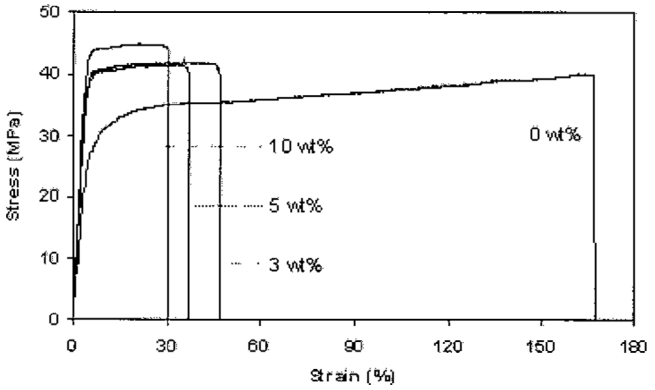

Figure 5: Representative stress-strain plots of neat PA 6,6 and PA 6,6-nHAp nanocomposites.

incorporation on the crystallization characteristics of melt-compounded PA 6,6-nHAp nanocomposites, we have subjected the nanocomposites to non-isothermal cycles in DSC. The crystallization temperatures (T_c), apparent melting temperatures (T_m) and the corresponding enthalpies (ΔH_c and ΔH_m) are reported in Table 2. The data indicate that, at concentrations of up to 10 wt%, nHAp does not have a considerable effect on the thermal characteristics of polyamide.

Effect of nHAp on the Thermal Stability of PA 6,6

The thermal stability of engineered polymers is of prime importance in fabrication processes. Knowledge gained from studies of polymer degradation may lead to more useful and stable products. Thermal degradation of polymers is a major problem at temperatures above the melting point and inevitably occurs in polymer melts during processing. The study of thermal degradation can be best complimented or corroborated by such techniques as thermogravimetric analysis (TGA) which measures the weight loss as a function of temperature, or the derivative TGA, i.e., DTG.

There are several reports in the literature regarding the enhancement of thermal stability of polymers containing nanofillers (e.g., nano silica, carbon

Table 2: DSC-determined thermal characteristics of PA 6,6-nHAp nanocomposites.

Concn. of nHAp (wt%)	T_c (°C)	ΔH_c (J/g)	T_m (°C)	ΔH_m (J/g)
0	228.7	34.1	262.4	46.0
3	227.9	33.5	262.9	43.8
5	227.9	32.3	263.2	44.8
10	228.2	30.2	262.8	43.5

nanotubes) [26–29]. Therefore, we have investigated the effect of hydroxyapatite nanoparticles on the thermal decomposition characteristics of polyamide. Figure 6(a) indicates the thermogravimetric traces of PA 6,6-nHAp nanocomposites. It is evident from the figure that the thermal stability of nHAp-reinforced nanocomposites is higher than that of neat PA 6,6. For example, the onset of thermal decomposition (temperature of 5% weight loss) of the nanocomposite sample containing 3 wt% nHAp is roughly 12°C higher as compared to neat PA 6,6. With further increase in nHAp concentration, the onset decomposition temperature increases further. Peak decomposition temperature values are also considerably higher for the nanocomposites as revealed from differential thermograms given in the Figure 6(b).

The improved thermal stability features of the nanocomposite samples are attributed to the effective interfacial interaction between the polymer matrix

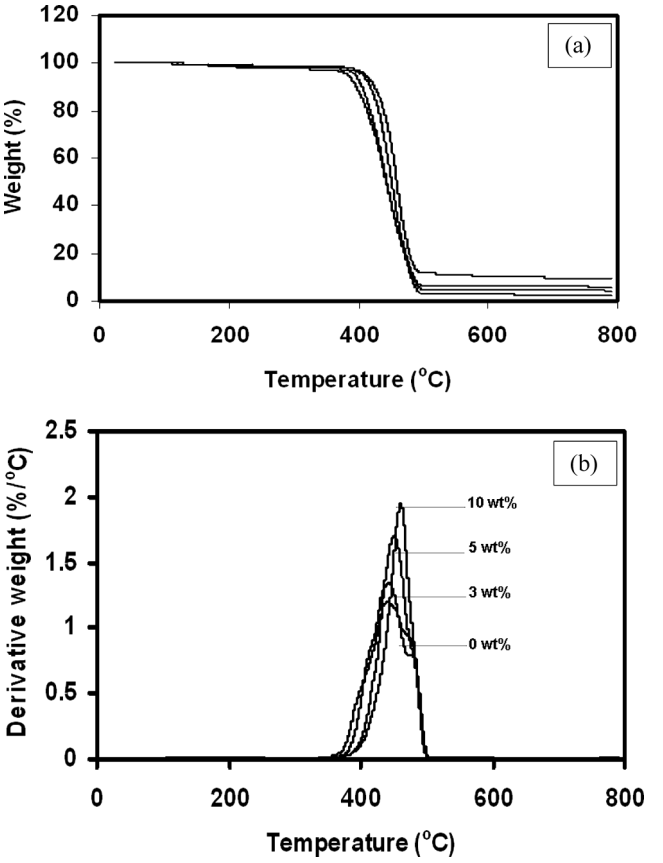

Figure 6: (a) TGA plots of neat PA 6,6 and PA 6,6-nHAp nanocomposites (Upper curves with increasing concentration of nHAp) (b) Effect of nHAp on the peak decomposition temperature of PA 6,6 (DTG traces).

Table 3: Effect of nHAp on the thermal decomposition of PA 6,6.

Concn. of nHAp (wt%)	Onset of thermal decomposition (°C)	Peak decomposition temperature (°C)
0	383.8	438.9
3	395.1	441.8
5	406.7	450.6
10	411.8	460.1

and the inorganic filler, which in turn points to a homogeneous filler dispersion. The onset of thermal decomposition and the peak decomposition temperature values are reported in Table 3.

CONCLUSIONS

Polyamide-nanohydroxyapatite nanocomposites have been prepared through melt compounding. The improved mechanical properties of the nanocomposites revealed that a small concentration of nHAp could substantially reinforce the matrix polymer well above that predicted by a continuum model that would be applicable to a microreinforced polymer. Melting and crystallization characteristics of the polyamide matrix remained almost unaltered with nanohydroxyapatite at low loading fractions. Thermogravimetric analysis indicated that hydroxyapatite nanoparticles considerably improved the thermal stability of PA 6,6.

REFERENCES

[1] Jarcho, M., Kay, J. F., Gumar, K. I., Doremus, R. H., and Drobeck, H. P. *J. Bioeng.* **1**, 79 (1977).

[2] Hollinger, J. O., and Battistone, G. C. *Clin. Orthop. Relat. Res.* **207**, 290 (1986).

[3] Peppas, N. A., and Langer, R. *Science* **263**, 1715 (1994).

[4] Damien, C. J., and Parson, J. R. *Appl. Biomater.* **2**, 187 (1992).

[5] Wang, M. *Biomaterials* **24**, 2133 (2003).

[6] Bonfield, W. *Met. Mater.* **3**, 712 (1987).

[7] Bonfield, W., Grynpas, M. D., Tully, A. E., Bowman, J., and Abram, J. *Biomaterials* **2**, 185 (1981).

[8] Wang, M., Hench, L. L., and Bonfield, W. *J. Biomed. Mater. Res.* **42**, 577 (1998).

[9] Fang, L., Leng, Y., and Gao, P. *Biomaterials* **26**, 3471 (2005).

[10] Fang, L., Leng, Y., and Gao, P. *Biomaterials* **27**, 3701 (2006).

[11] Teoh, S. H., Tang, Z. G., and Hastings, G. W. (1998). *Handbook of Biomaterial Properties*. J. Black and G. Hastings, Eds., Chapman & Hall, London, UK.

[12] Abubakar, M. M., Cheang, P., and Khor, K. A. *J. Mater. Process. Technol.* **89**, 462 (1999).

[13] Hong, Z., Zhang, P., He, C., Qiu, X., Liu, A., Chen, L., Chen, X., and Jing, X. *Biomaterials* **26**, 6296 (2005).

[14] Arostegui, S., Gay, S., and Lemaître, J. *European Cells and Materials* **13**, 8 (2007).

[15] Wei, J., Li, Y., and Lau, K. T. *Composites: Part B* **38**, 301 (2007).

[16] Wang, X., Li, Y., and Wei, J., and de Groot, K. *Biomaterials* **23**, 4787 (2002).

[17] Yi, Z., Yubao, L., Jidong, L., Xiang, Z., Hongbing, L., Yuanyuan, W., and Weihu, Y. *Materials Science and Engineering A* **452**, 512 (2007).

[18] Jie, W., and Yubao, L. *European Polymer Journal* **40**, 509 (2004).

[19] Wang, H., Yubao, L., Zuo, Y., Jihua, L., Ma, S., and Cheng, L. *Biomaterials* (2007) doi:10.1016/j.biomaterials.2007.04.014

[20] He, G., Dahl, T., Veis, A., and George, A. *Nat. Mater.* **2**, 552 (2003).

[21] Kumar, R., Prakash, K. H., Cheang, P., and Khor, K. A. *Langmuir* **20**, 5196 (2004).

[22] Cox, H. L. *British Journal of Applied Physics* **3**, 72 (1952).

[23] Halpin, J. C. *Journal of Composite Materials* **3**, 732 (1969).

[24] Callister, W. D., Jr. (2001). *Fundamentals of Materials Science and Engineering* Fifth Edition, John Wiley & Sons.

[25] Yang, F., and Nelson, G. L. *J. Appl. Polym. Sci.* **91**, 3844 (2004).

[26] Yang, S., Castilleja, J. R., Barrera, E. V., and Lozanoa, K. *Polymer Degradation and Stability* **83**, 383 (2004).

[27] Pötschke, P., Fornes, T. D., and Paul, D. R. *Polymer* **43**, 3247 (2002).

[28] Ou, C. F. *J. Appl. Polym. Sci.* **89**, 3315 (2003).

[29] Kashiwagi, T., Grulke, E., Hilding, J., Harris, R., and Awad, W. *J Macromol. Rapid Commun.* **23**, 761 (2002).